

Meteoroid Fragmentation as Revealed in Head- and Trail-echoes Observed with the Arecibo UHF and VHF Radars

J. D. Mathews · A. Malhotra

Abstract We report recent 46.8/430 MHz (VHF/UHF) radar meteor observations at Arecibo Observatory (AO) that reveal many previously unreported features in the radar meteor return—including flare-trails at both UHF and VHF—that are consistent with meteoroid fragmentation. Signature features of fragmentation include strong intra-pulse and pulse-to-pulse fading as the result of interference between or among multiple meteor head-echo returns and between head-echo and impulsive flare or “point” trail-echoes. That strong interference fading occurs implies that these scatterers exhibit well defined phase centers and are thus small compared with the wavelength. These results are consistent with and offer advances beyond a long history of optical and radar meteoroid fragmentation studies. Further, at AO, fragmenting and flare events are found to be a large fraction of the total events even though these meteoroids are likely the smallest observed by the major radars. Fragmentation is found to be a major though not dominate component of the meteors observed at other HPLA radars that are sensitive to larger meteoroids.

Keywords meteor radar · meteoroid fragmentation · meteor flare

1 Introduction

Here we provide an update to Mathews et al. (2010) who present Arecibo Observatory (AO) radar meteor results that are consistent with meteoroid fragmentation. While this conclusion has proven to be controversial; the finding that fragmenting meteoroids are observed both optically and with radar has a long history. In reference to fragmentation, Verniani (1969) notes that “At present, the structure and composition of meteoroids is a matter of controversy, with contrasting views put forward by different investigators.” In fact, Mathews (2004) notes evidence of meteoroid fragmentation and terminal flares dating to the first known radar meteor Range-Time-Intensity (RTI) image given in Hey et al. (1947) and in Hey & Stewart (1947). Additionally, there is much evidence and many papers on “gross fragmentation” in optical bolides – e.g., see Ceplecha et al. (1993) and references therein.

At the Meteoroids 2001 conference Elford & Campbell (2001) noted that “Radar reflections from meteor trails often differ from the predictions of simple models. There is a general consensus that these differences are probably the result of fragmentation of the meteoroid.” Elford (2004) concluded that approximately 90% of all specular trail events are accessible to his Fresnel holography approach while only about 10% of these events can be analyzed via the classical approach and thus that fragmentation is a dominant process for 80% of the specular trail events.

“Terminal” radar meteor events—referred to here as terminal flares—are reported in the Arecibo UHF/VHF results by Mathews (2004). Kero et al. (2008) report smooth to complex meteor light-curves

J. D. Mathews (✉) · A. Malhotra
Radar Space Sciences Lab, The Pennsylvania State University, University Park, PA USA 16802. Email: JDMathews@psu.edu

(their Figures 1-3) that they interpret as simple ablation, two-fragment, & multiple-fragment events with interference of the various head-echo signals. Roy et al. (2009) use genetic algorithm techniques to explore details of fragmenting meteors observed at the Poker Flat Incoherent Scatter Radar (PFISR). They employ multiple model point scatterers as we will outline below and a genetic algorithm to find via the evolution of three multi-fragment meteor events in a piece-wise fashion over groups of five radar pulse voltage (as opposed to power and thus lost phase information) returns finding the speed, deceleration, and amplitude of each particle in the ensemble. Their fitting procedure yields relative speed resolutions of as little as 1 m/s. Briczinski et al. (2009) utilize statistical techniques to estimate the role of fragmentation and terminal flares in Arecibo UHF radar meteor data. They find that terminal flares constitute up to ~15% of all events and that low-SNR, short duration, and/or fragmentation explain the ~67% of all events for which deceleration cannot be determined.

2 Observational Technique

The observations reported here utilize both the AO 430 MHz and 46.8 MHz radar systems. It is important to emphasize that these radars are frequency and time coherent and thus phase coherent over very long periods – years – and so in principle offer the ability to resolve features or motions on the scale of a fraction of a wavelength and centimeters/sec, respectively. These properties are utilized in the observations reported here. These two radars employ co-axial feeds yielding an overlapping central illuminated volume thus yielding a sizeable fraction of events that are seen in both radars. Table 1 lists the relevant parameters of both radars while Figure 1 shows the 430 MHz linefeed that illuminates the spherical-cap surface along with the four Yagi feeds arranged co-axially around the linefeed. At 46.8 MHz the dish is effectively parabolic allow this “point” feed arrangement. In Table 1 the quality factor is transmitter power (MW) time the effective area of the antenna (m²) divided by the system temperature (Kelvins). Clearly the UHF system is much more sensitive – by a factor of ~600 – than the VHF system.

Table 1. Arecibo V/UHF Radar Properties

Radar	Beamwidth	Gain (dBi)	Power	System Temp	Quality Factor
46.8 MHz	1.4°	40	~40 kW	3000 K	~3
430 MHz	0.17°	61	~2 MW	100 K	~1825

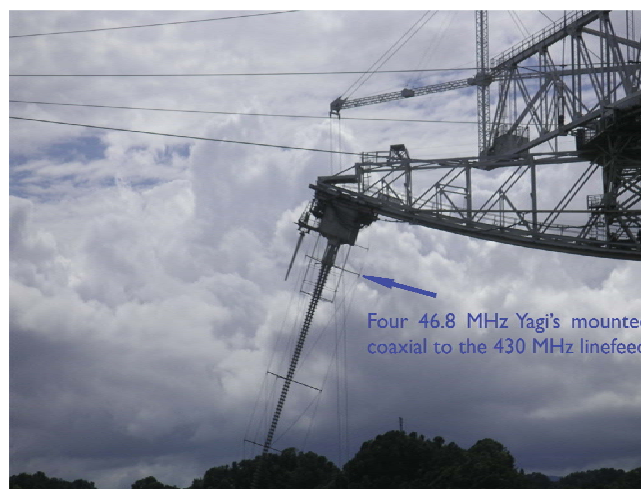


Figure 1. The VHF & UHF antenna feed layout of the AO carriage-house radars.

For the results given here a 20 μ sec uncoded pulse was used at UHF while – due to system duty cycle limitation – a 10 μ sec uncoded pulse delayed by 12 μ sec relative to the UHF pulse start was employed at VHF. In both cases the receive system bandwidth was 1 MHz while in-phase and quadrature samples were taken at baseband with 1 μ sec sampling intervals yielding 150 m range resolution. A 1 ms InterPulse Period (IPP) was utilized with the overall technique based on early AO D-region observations (Mathews 1984). The first dedicated AO meteor observations are reported by Mathews et al. (1997).

3 Observational Results

The results presented here were obtained during two \sim 12 hr observing sessions beginning at 2000 hr AST (Atlantic Standard Time) on 5 and 6 June 2008. Approximately 17,000 meteors were detected at UHF using automated detection software (Briczinski et al. 2009, Mathews et al. 2003, Wen et al. 2005, Wen et al. 2004). This approach was not separately applied at VHF due to the relatively short pulse and the high level of interference in the VHF band. The VHF results have been manually searched for large events that include some of the flare-trail results reported here.

Figure 2 displays Range-Time-Intensity (RTI) images of three meteor events that together characterize many of the \sim 17,000 UHF events we report here. Event 1, seen at 430 MHz, shows strong interference fading consistent with two slowly separating meteoroid fragments each of which has an individual head-echo. This interpretation builds on the results of Mathews et al. (2010) and Roy et al. (2009) and will be addressed further in the discussion section.

Event 2a, seen at VHF, shows several features including an underlying interference or fading pattern similar to event 1 but also an altitude-narrow trail that we attribute to an impulsive fragmentation “flare” occurring at about 40 ms and that results in a relatively small “blob” of plasma embedded in the background atmosphere. The term “flare” is adopted from optical meteor observations that often reveal impulsive brightening events. Event 2b shows the UHF return which defines the center of both beams. Note the strong intra-pulse fading that is due to the rapidly evolving particle distribution relative to the 69.7 cm wavelength. Figure 2, Event 3, shown only at VHF as the corresponding UHF event was very weak, shows mild fragmentation prior to 60 ms when a strong fragmentation flare occurs followed by a second flare at 110 ms. Of special interest in Event 3 is the strong interference fading – similar in effect to the Event 1 interference pattern – between the head-echo and trail-echoes. The implications of these various two-scatterer interference patterns will be explored in the discussion section and additional example events including those resembling differential ablation (Janches et al. 2009) and those opposite to differential ablation signature (intensity rises rapidly and falls slowly) are given in Mathews et al. (2010).

Next we consider some of the more subtle and perhaps surprising results from this dataset. Figure 3 displays a short UHF meteor head-echo that shows the beam pattern with a stronger central return and two side-lobe returns as the meteor moves across the beam. This event also displays a complex intra-pulse fading consistent with multiple, closely-spaced but rapidly dispersing, meteoroid “fragments” similar to those seen in Figure 2 event 2b, which is more slowly evolving (Roy et al. 2009). We are able to resolve these features of the meteoroid multi-head-echo evolution at the microsecond level due to the phase coherent nature of these radars. The Figure 3 VHF return is much longer than at UHF because – per Table 1 – the VHF beam is much wider. The combined U/VHF event is in common volume only over the span of the UHF return. The VHF meteor interference feature is simple like that of Figure 2, event 1 but fades more slowly than the Figure 3 UHF return as the wavelength is more than a factor of

nine longer. The VHF return displays a clear terminal flare that is consistent with the LATE (Low-Altitude Trail-Echo) reported at Jicamarca (Malhotra & Mathews 2009). This type of event is relatively common.

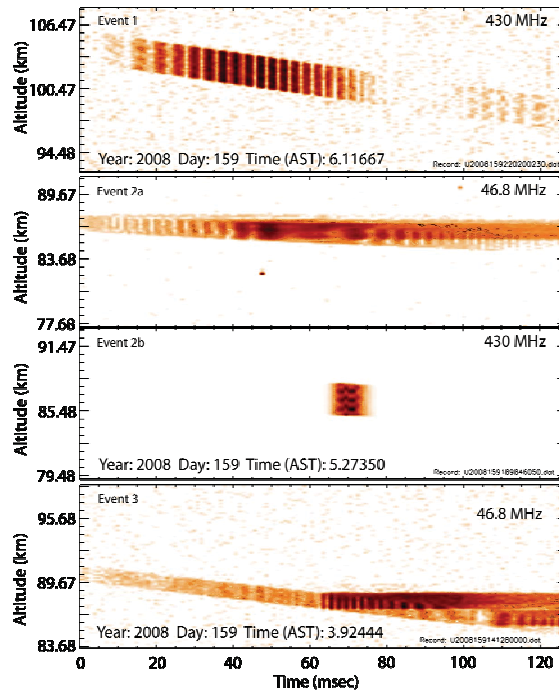


Figure 2. RTI images of three archetypal AO meteor events. Event 1, seen at UHF, shows a strong fading pattern consistent with two slowly separating meteoroid fragments each of which has an individual head-echo. The event 2 panels demonstrate the value of viewing the same event at two widely separated frequencies. Event 2a, seen at VHF, shows several features including an underlying interference pattern similar to event 1 but also an altitude-narrow trail that we attribute to a fragmentation “flare”. Event 3 shows some Event 1 like fragmentation and two flare-trails. (Fig. 1 from Mathews et al. (2010))

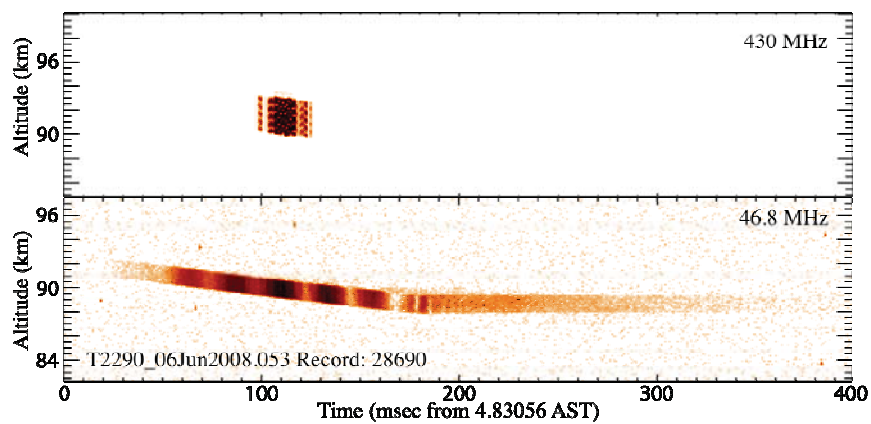


Figure 3. RTI images of a meteor event seen at both UHF and VHF. The UHF head-echo shows the beam-pattern as strong intra-pulse fading. The VHF echo has a terminal flare.

Figure 4 shows two UHF meteor events that are ambiguous and thus point to the wide range of knowledge potentially available via radar meteor studies. Event 1 is likely due to two or more particles that cause the strong intra-pulse interference fading visible in the ~60-70 IPP and ~82-95 IPP. It is unclear if the early event results in a trail and is then followed by a separate event that clearly results in the UHF trail. In any case, we might deem this total event a nano-shower in that almost certainly all particles were associated with a parent body at or just above atmospheric entry. Figure 4 event 2 is likely a terminal flare trail event similar to those reported at the 1280 MHz Sondrestrom Research Facility (SRF) terminal events (Mathews et al. 2008). It is also possible that this event is a “classical” trail event where the trajectory of the meteoroid is perpendicular to the zenith-pointing beam.

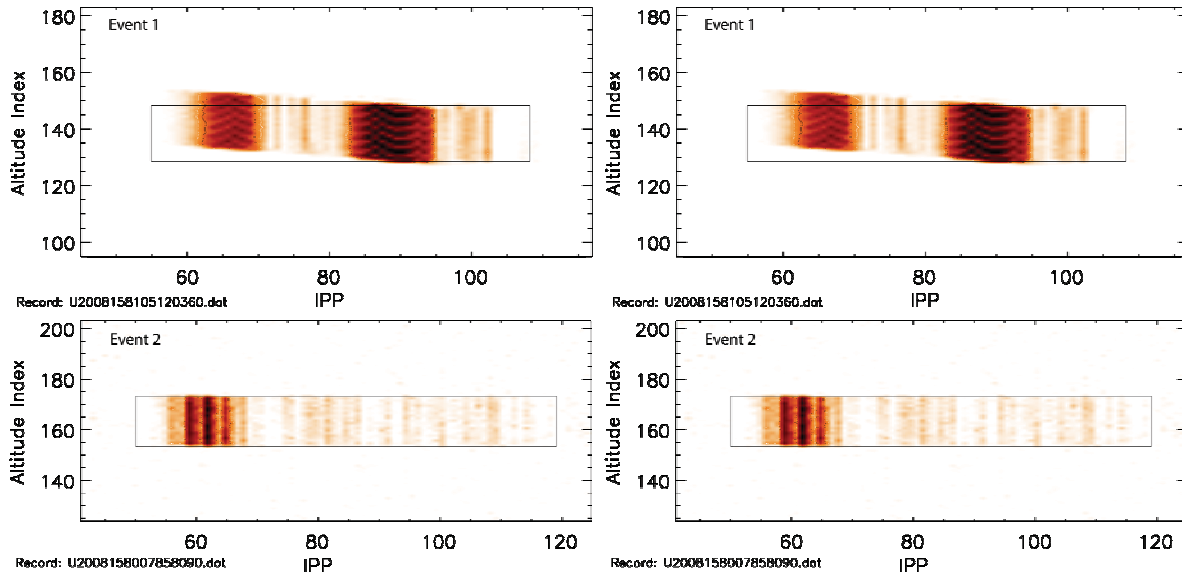


Figure 4. RTI images of two complex UHF head- and/or trail-echo events. Event 1 shows strong intra-pulse fading due to two or more individual head-echo producing meteoroids in close proximity. Event 1 displays a clear trail-echo after IPP 95. Event 2 is likely a terminal-flare trail but may be a classical trail-echo where the trajectory of the meteoroid is perpendicular to the zenith-pointing beam.

Figure 5 points to a new – previously unreported – class of radar meteor event. These long-lasting – for $k\angle B \approx 45^\circ$ – trail events appear to be the “fossil” remnants of a radar bolide event. That is, while the head-echo of the progenitor event is not always identifiable, the event generated sufficient (flare?) trail-producing plasma that the resultant trail-echo lasts a few seconds and may in fact drift into the VHF beam at the normal D-region wind speeds of order 100 m/s (Mathews 1976). Note the complex interference fading of the several regions of the trail-plasma.

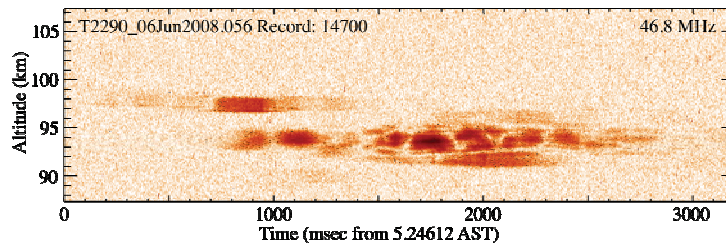


Figure 5. A likely “fossil” radar bolide event that has an ~3 sec lifetime. The progenitor event was not observed.

4 Discussion

We report several classes of V/UHF “common volume” radar meteor events that are, we argue, consistent with fragmenting meteoroids that produce multiple, interfering, head-echo events as well as “flare” and “terminal flare” trails that often display interference fading between/among the head- and trail-echo components. That fading occurs in a simple pattern (e.g., similar to the classic Young’s point-source optics experiment) suggests a simple model of the meteor scattering process that, as we show below, appears both necessary and sufficient to explain what we observe. It is important to stress in introducing this model that it is successful in part due to the time and frequency and thus phase coherence of both the VHF and UHF radars that permit full use of the model we present. We also note that this capability has been intrinsic to most radars for many years but that full advantage of this “holographic” capability is just beginning for the modern geophysical radars.

In the model scenario we propose, each head- or trail-echo signal is consistent with a point target – i.e., each has a well-defined phase center – that is readily modeled at the receiver baseband as

$$x_n(t) = A_n \exp\left(\frac{j4\pi R_n(t)}{\lambda}\right) \quad (1)$$

where $R_n(t) = R_n(t_0) - v_n(t - t_0) + d_n(t - t_0)^2 / 2$ – the subscript n refers to the n th meteoroid fragment. In (1), $j = \sqrt{-1}$ and the multiple meteoroid fragments are taken to be traveling on the same trajectory at range $R_n(t)$ time t with t_0 the initial time and with constant speed and deceleration v_n, d_n , respectively. It is important to note that equation (1) is accurate only if all the meteor energy is contained in the received bandwidth at baseband – otherwise filter features such as ringing may occur. To this end we employ a 1 MHz bandwidth (actually 0.5 MHz at baseband for both the in-phase and quadrature channels thus satisfying the Nyquist sampling condition), 1 μ s sample intervals, and a transmitter pulse of 10/20 μ s at VHF/UHF, respectively. Thus the pulse spectrum is very narrow with respect to the sampled bandwidth so that the meteor Doppler shift (~ 22 kHz at VHF and ~ 200 kHz at UHF for a 72 km/s meteor) does not result in signal energy being lost outside the filter bandpass. Also note that eqn. (1) embodies the Doppler shift of the spectrum via the time rate of change of $R(t)$ within a given pulse.

In an example of the successful use of equation (1), it can be seen that the signals from two slowly separating fragments alternately appear in- and out-of-phase as the net path from the two particles to the receiver varies over half a wavelength, $\lambda/2$. This results in a Young’s experiment-like outcome as we demonstrate below. Use of (1) to successfully characterize meteor head-echo returns and extract Doppler information dates to the earliest meteor observations at Arecibo Observatory (Janches et al. 2003, Mathews et al. 2003, Mathews et al. 1997). Radio science implications are discussed by Mathews (2004).

Figure 6 bottom panel shows Figure 2, event 1 along with modeling results that employ eqn. (1) for two particles (head-echoes) at both AO radar frequencies. The model results include Gaussian distributed random noise in both the in-phase and quadrature channels. As noted in the caption, the two particles are taken to start together but then separate at speeds of 50.4 km/s and 50.3 km/s, respectively, with no deceleration. The particle head-echoes have equal scattering cross-sections. The model beam-pattern at UHF is modeled as a double Gaussian yielding main- and side-lobes that closely match the observed meteor return. The VHF beam-pattern is a single very wide Gaussian that causes slight intensity decrease at the model event edges.

The Figure 6 model results at 430 MHz are completely consistent with the observations. The matching could be “tuned” by adjusting the speeds, adding a slight deceleration, and adjusting the initial

phase separations of the two particles. However, this complexity is unnecessary and will be left to actual multi-particle fitting algorithms (Briczinski et al. 2006) that are currently under development for the multi-particle case. Mathews et al. (2010) gives a similar modeling/data comparison but for head-echo fading with a stationary flare-trail while Roy et al. (2009) give details on using equation (1) fitting via genetic algorithms. The VHF model result in Figure 6 shows the slower fading rate at VHF relative to UHF. This model result is similar to the observational results given in Figure 3 where the UHF fading rate is very rapid while the VHF fading rate is quite similar to the Figure 6 VHF model result.

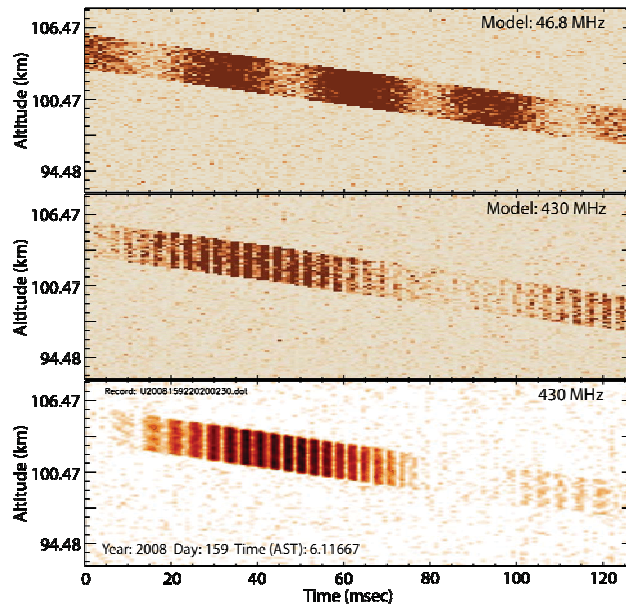


Figure 6. RTI images of an observed and modeled two-particle meteor event. The bottom panel event is just Figure 2, event 1. The model is eqn. (1) applied separately to two particles of equal scattering cross-section that start at the same location but separate as the speeds are taken to be 50.3 km/s and 50.4 km/s with no deceleration. The VHF and UHF fading rates are different due to the much longer wavelength (6.4 m vs. 0.697 m) at VHF. See text for details on the beam-patterns.

5 Conclusions

We have reported on common volume V/UHF radar meteor observations at Arecibo Observatory. These observations have revealed meteor head- and trail-echo features that are consistent with meteoroid fragmentation. Further, the VHF observations have revealed flare-related trail-echoes that, due to the interference fading between the head- and trail-echoes, are found to be “small” compared with a wavelength in that a well defined phase center exists. We additionally find that both a necessary and sufficient description of the head- and trail-echoes is given by eqn. (1) which simply models point-target scattering at receiver baseband with no Doppler spreading of the spectrum as this has not proven necessary. We give modeling results supporting this conclusion. These results go beyond those given by Mathews et al. (2010) and Roy et al. (2009) and provide necessary insight into the radio science aspects of radar meteor observations (Mathews 2004).

We additionally report observations of UHF trail-echoes and UHF meteor echoes that are consistent with meteoroid terminal “flare” events and/or “classical” meteor echoes from a meteor traveling perpendicular to the radar pointing direction that is at zenith for these results. Also, we report

what may be a new class of radar meteor events that we term “radar bolides”. Thus far, radar bolides appear only as large (i.e., intense, distributed in altitude, and long-lived) trail-events in that the progenitor meteoroid head-echo has not been convincingly identified as it apparently falls outside the radar beam. The radar bolides last 100’s of milliseconds through, thus far, to about 10 seconds and consist of multiple scattering centers distributed over several kilometers in range. Apparently these “trails” drift into the radar beam due to the ~100 m/s winds in the upper mesosphere (Mathews 1976). It seems likely that this pattern of scatterers is formed when a large meteoroid breaks into a pattern of still large meteoroids with significant horizontal dispersion at 90 km altitude where we observe the “radar bolide” event. In any case, the “radar bolide” is quite intensive relative to the usual meteor events.

While Mathews et al. (2010) reports ~90% fragmentation signatures for this set of observations, a companion paper (Malhotra and Mathews, these proceedings), report a different distribution of meteor events from the Resolute Bay Incoherent Scatter Radar (RISR). At RISR they find an event type distribution of fragmentation (48%), simple ablation (32%), and differential ablation (20%). We suggest that this contrast is likely caused by AO “seeing” significantly smaller meteoroids than RISR – this due to the much higher sensitivity of AO relative to RISR.

Finally we note that the simultaneous presence of close meteoroid fragments renders a clear definition of dynamic mass (Fentzke et al. 2009, Janches & Chau 2005, Mathews et al. 2001), absolute scattering-cross section mass (Close et al. 2005), and meteoroid mass density (Briczinski et al. 2009, Novikov & Pecina 1990) difficult at best. Additionally, interpretation of details such as differential ablation (Janches et al. 2009) also becomes difficult as the ensemble of evolving particles appears to be capable of producing not only the lightcurves we expect for a differential ablation event but also the exact opposite (Mathews et al. 2010; Malhotra and Mathews, these proceedings). Put concisely, our results indicate that many meteoroids arrive at the top of the atmosphere as a “dustball” or an otherwise loosely-attached configuration of particles (Verniani 1969) that begin to separate immediately on encountering the atmosphere and/or as the system proceeds into the atmosphere and becomes visible as a radar meteor. These particles also undergo occasional instantaneous “flaring” whereby one of the ensemble of particles or a newly created particle is apparently terminally destroyed thus creating the plasma “blob” that we observe as the flare.

To paraphrase (Verniani 1969), the authors wish to conclude this section by quoting the thoughts of one of the historically-most-established leaders in meteor research: “I regard the process of fragmentation of meteor bodies as even more important than is recognized now. Therefore further studies of this process seem to be necessary. It is impossible to predict the course of fragmentation for an individual meteor particle but statistical regularities of the fragmentation process must exist and they should be studied. These statistical regularities are probably somewhat different for different meteor streams and also probably vary with the mass of the meteor particles.” (Levin 1968)

Acknowledgements

The Arecibo Observatory is part of the National Astronomy and Ionosphere Center, which is operated by Cornell University under a cooperative agreement with the National Science Foundation. This effort was supported under NSF grant ATM 07-21613 to The Pennsylvania State University.

References

- S.J. Briczinski, J.D. Mathews, & D.D. Meisel, *J. Geophys. Res.*, **114** A04311 (2009)
- S.J. Briczinski, C.-H. Wen, J.D. Mathews, J.F. Doherty, & Q.-N. Zhou, *IEEE Trans. Geos. Remote Sens.*, **44** 3490 (2006)
- Z. Cepelcha, P. Spurny, J. Borovicka, & J. Keclikova, *Astron. Astrophys.*, **279** 615 (1993)
- S. Close, M. Oppenheim, D. Durand, & L. Dyrud, *J. Geophys. Res.*, **110** A09308 (2005)
- W.G. Elford, *Atmos. Chem. Physics*, **4** 911 (2004)
- W.G. Elford, & L. Campbell, Effects of meteoroid fragmentation on radar observations of meteor trails, *Meteoroids 2001 Conference*, ESA Publications, **SP-495**, ed. B. Warmbein (Swedish Institute of Space Physics, Kiruna, Sweden, 2001) pp. 419-423
- J.T. Fentzke, D. Janches, & J.J. Sparks, *J. Atmos. Solar-Terr. Phys.*, **71** (2009)
- J.S. Hey, S.J. Parsons, & G.S. Stewart, *Mon. Not. R. Astron. Soc.*, **107** 176 (1947)
- J.S. Hey, & G.S. Stewart, *Proc. Phys. Soc. Lond.*, **59** 858 (1947)
- D. Janches, & J.L. Chau, *J. Atmos. Solar-Terr. Phys.*, **67** (2005)
- D. Janches, L.P. Dyrud, S.L. Broadley, & J.M.C. Plane, *Geophys. Res. Lett.*, **36** L06101 (2009)
- D. Janches, M.C. Nolan, D.D. Meisel, J.D. Mathews, Q.-H. Zhou, & D.E. Moser, *J. Geophys. Res.*, **108** 1-1 (2003)
- J. Kero, C. Szasz, A. Pellinen-Wannberg, G. Wannberg, A. Westman, & D.D. Meisel, *Geophys. Res. Lett.*, **35** (2008)
- B.Yu. Levin, Meteor Physics (Round-Table Discussion and Summary), *Physics and Dynamics of Meteors*, International Astronomical Union. Symposium no. 33, Dordrecht, D. Reidel, **33**, ed. L. Kresak, & P. M. Millman (Tatranska Lomnica, Czechoslovakia, 4-9 September, 1968) pp. 511-517
- A. Malhotra, & J.D. Mathews, *Geophys. Res. Lett.*, **36** L21106 (2009)
- J.D. Mathews, *J. Geophys. Res.*, **81** 4671 (1976)
- J.D. Mathews, *J. Atmos. Terr. Phys.*, **46** 975 (1984)
- J.D. Mathews, *J. Atmos. Solar-Terr. Phys.*, **66#3** 285 (2004)
- J.D. Mathews, S.J. Briczinski, A. Malhotra, & J. Cross, *Geophys. Res. Lett.*, **37** L04103 (2010)
- J.D. Mathews, S.J. Briczinski, D.D. Meisel, & C.J. Heinselman, *Earth, Moon, Planets.*, **102** 365 (2008)
- J.D. Mathews, J.F. Doherty, C.-H. Wen, S.J. Briczinski, D. Janches, & D.D. Meisel, *J. Atmos. Solar-Terr. Phys.*, **65** 1139 (2003)
- J.D. Mathews, D. Janches, D.D. Meisel, & Q.-H. Zhou, *Geophys. Res. Lett.*, **28** (2001)
- J.D. Mathews, D.D. Meisel, K.P. Hunter, V.S. Getman, & Q. Zhou, *Icarus*, **126** 157 (1997)
- G.G. Novikov, & P. Pecina, *Bul. Astron. Inst. Czechosl.*, **41** 387 (1990)
- A. Roy, S.J. Briczinski, J.F. Doherty, & J.D. Mathews, *IEEE Geosci. Remote Sens. Lett.*, **6** 363 (2009)
- F. Verniani, *Space Sci. Rev.*, **10** 230 (1969)
- C.-H. Wen, J.F. Doherty, & J.D. Mathews, *J. Atmos. Solar-Terr. Phys.*, **67** 1190 (2005)
- C.-H. Wen, J.F. Doherty, J.D. Mathews, & D. Janches, *IEEE Trans. Geos. Remote Sens.*, **42** 501 (2004)